

## Supplementary Material (ESI) for Journal of Materials Chemistry C

This journal is © The Royal Society of Chemistry 2012

### Supplementary Information

#### Templated One-step Catalytic Fabrication of Uniform Diameter

#### $Mg_xB_y$ Nanostructures

Fang Fang,<sup>a</sup> EswaramoorthiIyyamperumal,<sup>a</sup> Miaofang Chi,<sup>b</sup> GayatriKeskar,<sup>a</sup> Magdalena Majewska,<sup>a</sup>

Fang Ren,<sup>a</sup> Changchang Liu,<sup>a</sup> Gary L. Haller,<sup>a</sup> Lisa D. Pfefferle<sup>\*a</sup>

<sup>a</sup> Department of Chemical Engineering, Yale University, 9 Hillhouse Ave, New Haven, CT 06520

<sup>b</sup> Oak Ridge National Laboratory Materials Science Division 1 Bethel Valley Rd Oak Ridge TN 37830.

\*lisa.pfefferle@yale.edu

**HPCVD reactor.** The schematic set up of the HPCVD reactor is illustrated in Figure

S1.

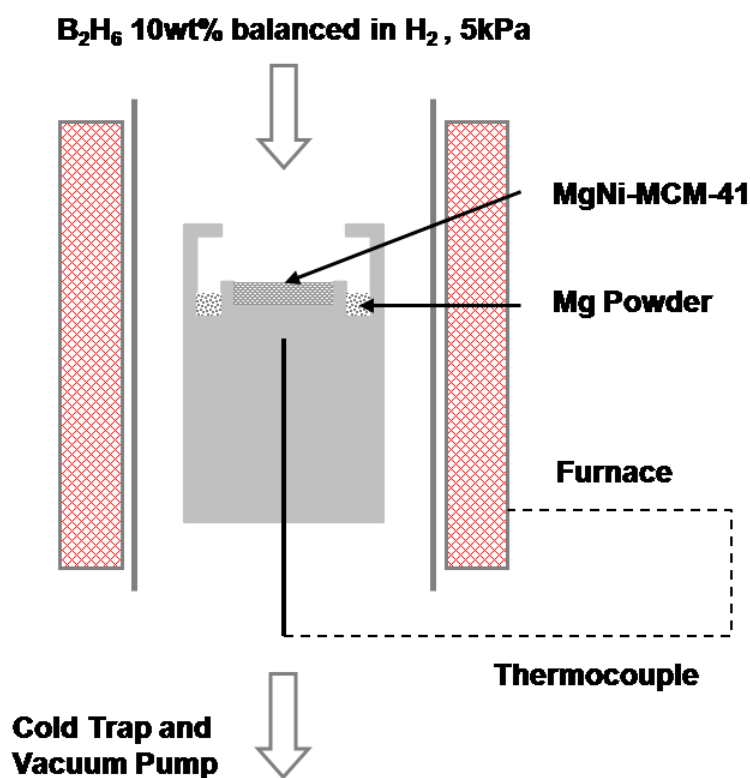


Figure S1: HPCVD Reactor Design

## Supplementary Material (ESI) for Journal of Materials Chemistry C

This journal is © The Royal Society of Chemistry 2012

**Structural Optimization of the Metal-incorporated MCM-41.** The physical structure of the bimetallic catalyst MgNi-MCM-41 was assessed by nitrogen physisorption as shown in Figure S2. The isotherm of our as-synthesized catalyst is reversible and shows no hysteresis, which is typical for well-ordered MCM-41 structures and in good agreement with previous reports on metal incorporated MCM-41.<sup>1,2</sup> Ideally, MCM-41 with one dimensional uniform diameter pores should exhibit a step jump of infinite slope in the isotherm because of uniform capillary condensation. The relative pressure where the jump appears corresponds to the specific pore diameter. Therefore, the uniformity of the mesopores can be characterized by the transition slope of the isotherm. Our as-synthesized MgNi-MCM-41 shows a steep jump around the relative pressure of 0.35, which indicates highly ordered uniform pore structures are achieved within our sample. The pore size distribution is further analyzed by the BJH method on the desorption isotherm, as shown in Figure S2b. The narrow pore size distribution, peak at 2.87nm with the full width at half-maximum about 0.2nm, further confirms the structures are well-ordered, similar to previous work from our group on pure Ni-MCM-41.<sup>2</sup> While Mg substitutes for the Si incorporated in the silica framework, it does introduce some degree of disorder in the MCM-41 framework. The BET surface area reduces almost linearly with increasing Mg loading (Figure S3).

## Supplementary Material (ESI) for Journal of Materials Chemistry C

This journal is © The Royal Society of Chemistry 2012

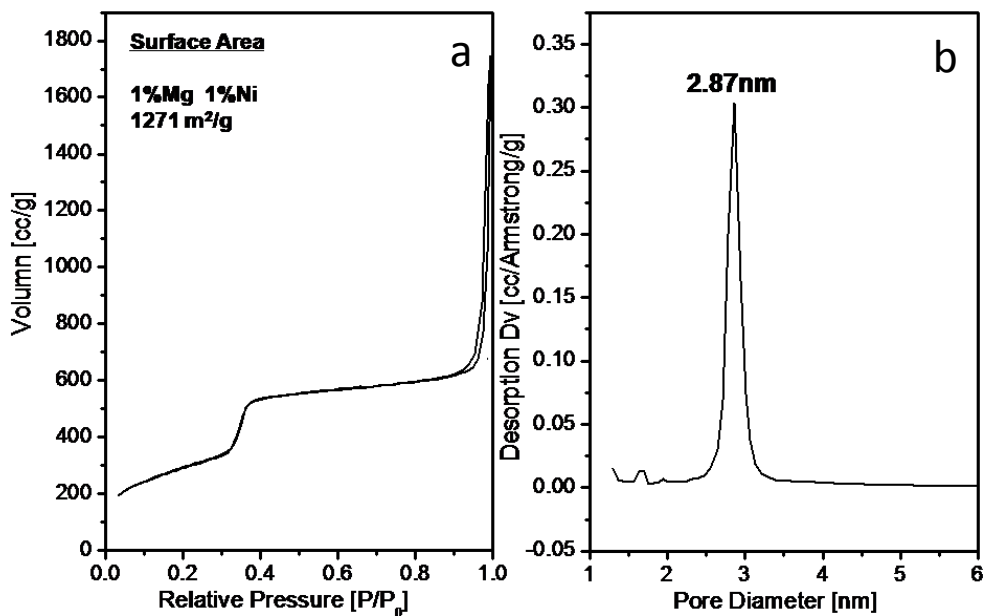


Figure S2: (a) Nitrogen Isotherm of the MgNi-MCM-41, (b) Pore size distribution of the MgNi-MCM-41 calculated by BJH method.

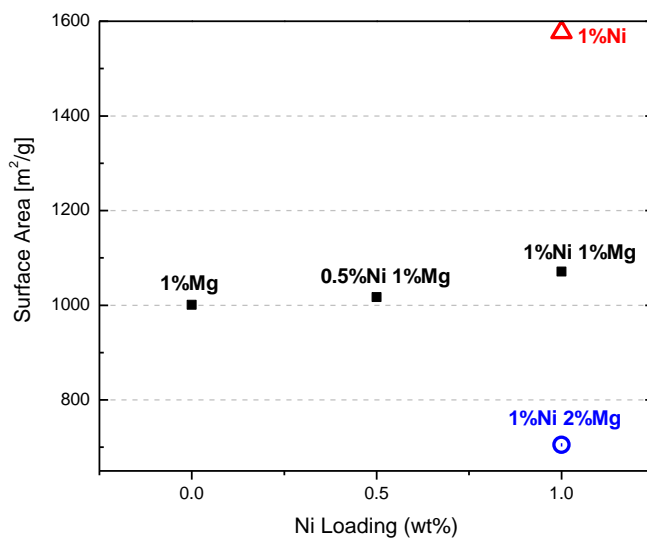


Figure S3: BET surface area comparison between different bi-metallic metal loadings.

## Supplementary Material (ESI) for Journal of Materials Chemistry C

This journal is © The Royal Society of Chemistry 2012

**Raman characterization on the as-synthesized  $Mg_xB_y$  samples.** As a complementary experiment to further investigate the effect of reaction temperature, Raman spectra were collected for the as-synthesized samples at two excitation wavelengths 785nm (Figure S4) and 532nm (Figure S5). With increasing reaction temperature, a narrow band centered at  $532.4\text{cm}^{-1}$  starts to show up in the associated Raman spectra excited at 785nm. For reactions below  $600^\circ\text{C}$ , no fabrication is observed under TEM, and correspondingly no band is resolved at  $532.4\text{cm}^{-1}$ . With the higher yield of  $Mg_xB_y$  nanostructures at higher reaction temperature, the intensity of the  $532.4\text{cm}^{-1}$  band also increases. Similarly, in Raman spectra excited at 532nm, a  $507.5\text{cm}^{-1}$  band was observed with increasing intensity along with the increasing reaction temperature. The discrepancy between the characteristic band positions under the two excitation wavelengths results from the different laser power applied during the measurements. For 532nm laser line, a fully open laser was used, and for 785nm laser line, a laser with OD3 of less laser power was used on the Jasco Raman Spectrometer. The higher laser power overheats the sample, leading to a red-shift in the corresponding measurement.<sup>3</sup> Comparison of the spectra under different laser power excited at 532nm indicates the red-shift range from fully open to a reduced openness of OD3 is  $24\text{cm}^{-1}$ .

Debate on the origin of this sharp band appearing in the range of  $500\text{cm}^{-1}$  -  $540\text{cm}^{-1}$  has continued for decade, which was detected in elemental boron using different instruments and exciting frequencies.<sup>4-6</sup> Weber and Thorpe<sup>7</sup> considered the very sharp

## Supplementary Material (ESI) for Journal of Materials Chemistry C

This journal is © The Royal Society of Chemistry 2012

525 $\text{cm}^{-1}$  Raman band (using 514.5nm laser excitation) “spurious” and excluded it from their discussion. Beckel et al.<sup>8</sup> utilized the valence-force field model to decipher this 525 $\text{cm}^{-1}$  band in elemental boron, and argued that this band arose from defected icosahedral boron cages, such as truncated  $\text{B}_{11}$  cages in an open manner. They claimed that the vacancy defects created by missing boron atoms would alter the electronic state and make possible a Raman transition between two electronic states with 0.0650eV difference in their ground vibrational states. A possible surface contamination or surface structural difference from the bulk phase was also speculated to be the cause. In the present study, the intensity of the 532.4 $\text{cm}^{-1}$  Raman band (while excited at 785nm) increases as reaction temperature rises. The trend is consistent with the enhancement of the 186.2eV pre-peak intensity in the boron K-edge spectra. The Raman spectra of the as-synthesized samples are compared with reference samples at two excitation wavelengths. When using 785nm laser excitation, the 532.4 $\text{cm}^{-1}$  Raman band is not present in the Mg powders or the MgNi-MCM-41 catalyst, which suggests this particular Raman band results from the reaction product. Moreover, the bulk phase  $\text{MgB}_2$  also does not have sharp band in the range of 100 $\text{cm}^{-1}$  – 1800 $\text{cm}^{-1}$ , indicating our as-synthesized  $\text{Mg}_x\text{B}_y$  has a structure distinguished from the bulk phase  $\text{MgB}_2$ . A small 525.3 $\text{cm}^{-1}$  Raman band (785nm laser excitation) is shown in the cleaned boron nanotube (BNT) sample with a small red-shift from the 750 $^\circ\text{C}$  as-synthesized  $\text{Mg}_x\text{B}_y$  nanostructures. The Raman spectrum of the purified BNT sample also has features in the range of 600 $\text{cm}^{-1}$  – 1300 $\text{cm}^{-1}$

## Supplementary Material (ESI) for Journal of Materials Chemistry C

This journal is © The Royal Society of Chemistry 2012

which represent the  $A_{1g}$  modes in icosahedral boron lattice.<sup>4, 8</sup> This is because significant amount of bulk phase boron was formed as a by-product during the CVD synthesis of pure boron nanotubes. Since there is no boron icosahedral lattice vibrational mode shown above  $600\text{cm}^{-1}$  in our spectra of the as-synthesized samples, we proposed that in the concentric tubular structure of  $\text{Mg}_x\text{B}_y$  the curvature of the boron layer could make the local coordination of boron closer to an opened defected icosahedral boron cage, which would explain why the  $532.4\text{cm}^{-1}$  Raman band is only present in the spectra of  $\text{Mg}_x\text{B}_y$  nanostructures but not the spectrum of bulk phase  $\text{MgB}_2$ . The red-shift between the purified BNT sample and the as-synthesized  $\text{Mg}_x\text{B}_y$  nanostructures could result from the different surface conditions.  $\text{Mg}_x\text{B}_y$  nanostructures have a layer of Mg on top (or two layers on both sides) of the boron tubular sheets, which shifts the electronic state of boron. Tallent et al.<sup>4</sup> argued that the  $534\text{cm}^{-1}$  band shown in the spectrum of boron carbide (514.5nm laser excitation) was associated with the CBC chain structures linking the  $\text{B}_{11}\text{C}$  cages, and suggested that the narrow bandwidth and the strong intensity indicates that the chains are well ordered. They also presented the Raman spectra of boron arsenide with a  $508\text{cm}^{-1}$  band and boron phosphide with a  $518\text{cm}^{-1}$  band collected under the same laser excitation of 514.5nm, both of which might have an origin similar to the  $525\text{cm}^{-1}$  band in rhombohedral boron. This indicates that boride compounds with different heteroatoms (such as As, P and C) could have a small shift in Raman bands, and suggests that the shift between  $\text{Mg}_x\text{B}_y$  nanostructures and purified boron nanotubes is

## Supplementary Material (ESI) for Journal of Materials Chemistry C

This journal is © The Royal Society of Chemistry 2012

in a reasonable range. Furthermore, there is no Raman band reported in the range of  $500\text{cm}^{-1}$  -  $540\text{cm}^{-1}$  for boron oxide<sup>9</sup> or boron nitride<sup>10</sup>, eliminating the possibility that this Raman band is induced by boron oxide or boron nitride. Therefore, we tentatively speculate that the  $534.2\text{cm}^{-1}$  Raman band at 785nm laser excitation ( $507.5\text{cm}^{-1}$  Raman band at 532nm laser excitation) results from the electronic state transition of boron in  $\text{Mg}_x\text{B}_y$  nanostructures with the concentric layer-by-layer structure, and there is urgent importance to theoretically model the Raman spectrum of  $\text{Mg}_x\text{B}_y$  nanotubes to prove (or disprove) our proposition.

## Supplementary Material (ESI) for Journal of Materials Chemistry C

This journal is © The Royal Society of Chemistry 2012

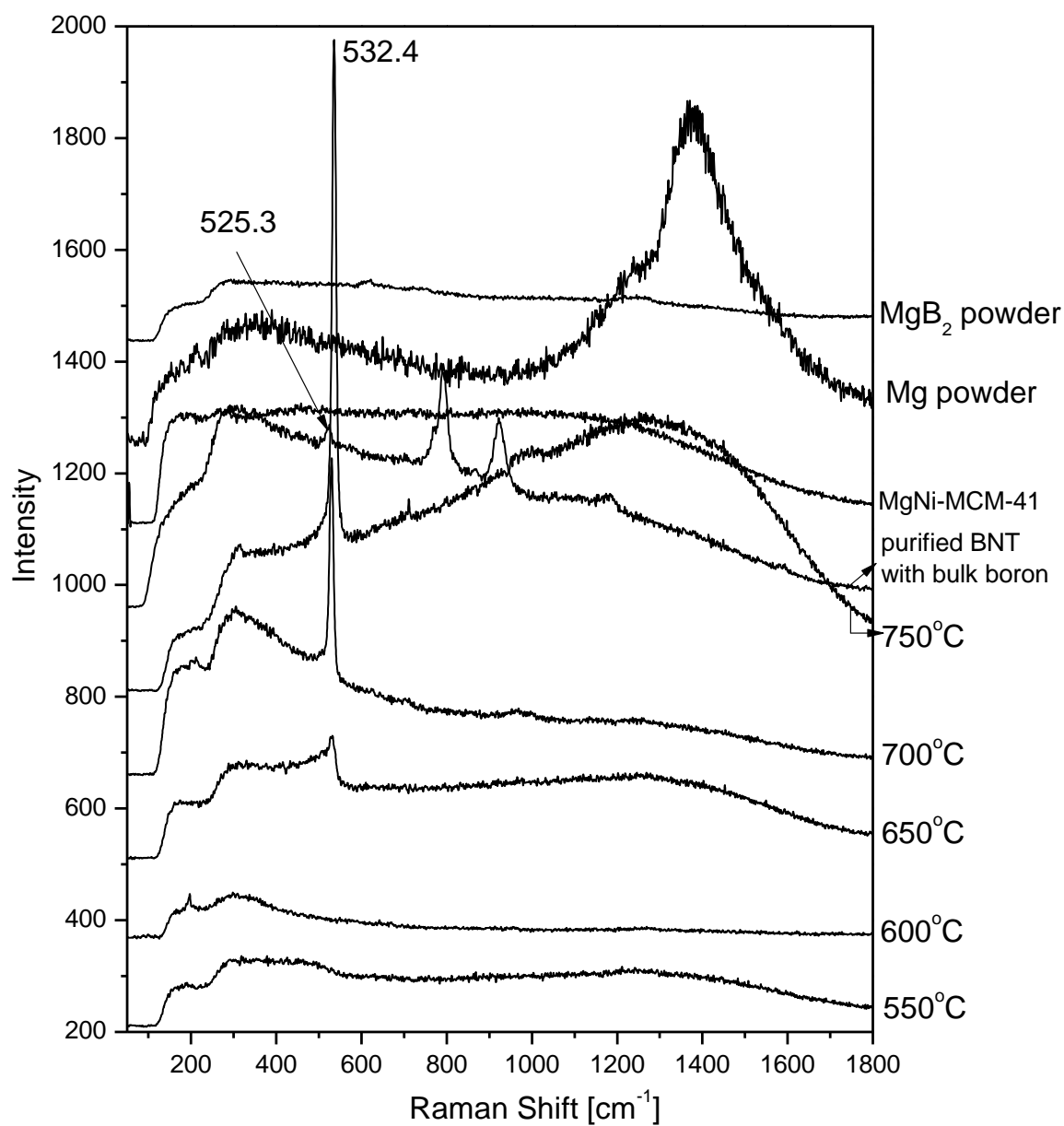


Figure S4: Raman spectra of the as-synthesized samples from different reaction temperatures measured at 785nm excitation.

## Supplementary Material (ESI) for Journal of Materials Chemistry C

This journal is © The Royal Society of Chemistry 2012

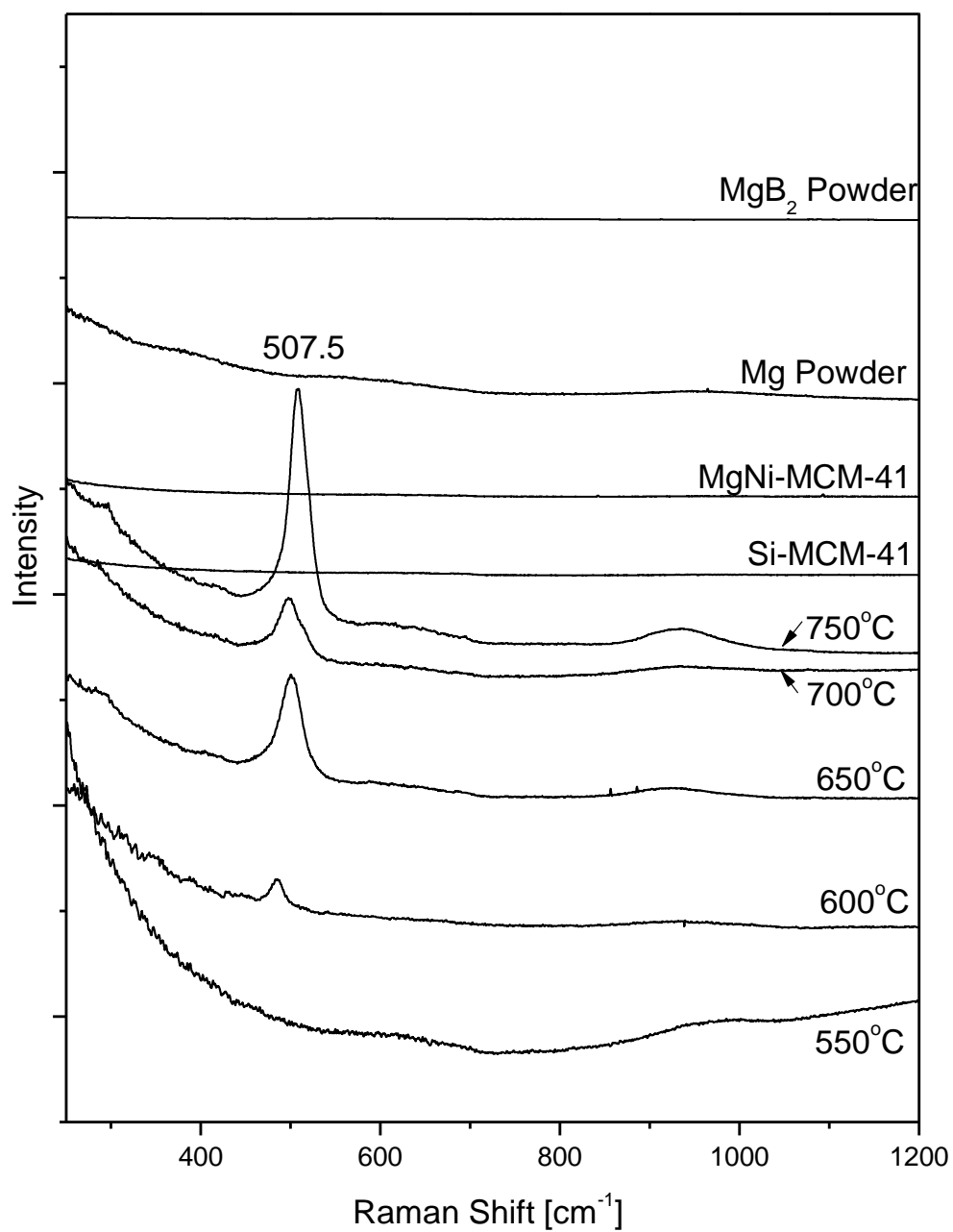


Figure S5: Raman spectra of the as-synthesized samples from different reaction temperatures measured at 532nm excitation.

## Supplementary Material (ESI) for Journal of Materials Chemistry C

This journal is © The Royal Society of Chemistry 2012

**DC magnetization of the as-synthesized  $Mg_xB_y$  nanostructures.** Different magnetic fields (0.003, 0.01, 0.1, 1.0 and 5.0 T) were applied to the sample. The sample was cooling down from room temperature to 7K under zero applied field. Then certain magnetic field was applied at this low temperature, and the longitude moment was measured with the increasing temperature. The Figure S6 presents the zero field cooling curves of the 750°C as-synthesized sample. The sharp diamagnetic transition around 40K suggests the existence of the  $Mg_xB_y$  layered structures. With increasing applied magnetic field, the drop of DC susceptibility is decreasing, as well as the diamagnetic transition temperature. A fine scan around the transition point indicates the  $T_C$  measured at 100 Oe applied magnetic field is 38.5K. It should be noted that the fine-scan figure on the top-left corner is a re-measurement in smaller temperature steps (0.5K) to accurately measure the transition temperature at 100Oe. While in broad comparison across different applied magnetic fields, the measurements were taken at 5K temperature increment. The slight signal difference could come from using a finer step size. This transition signal diminishes when the applied magnetic field is higher than 1 T. The concentration of the active diamagnetic component, i.e.  $Mg_xB_y$  nanostructures, in the as-synthesized sample is about 0.02wt%.

## Supplementary Material (ESI) for Journal of Materials Chemistry C

This journal is © The Royal Society of Chemistry 2012

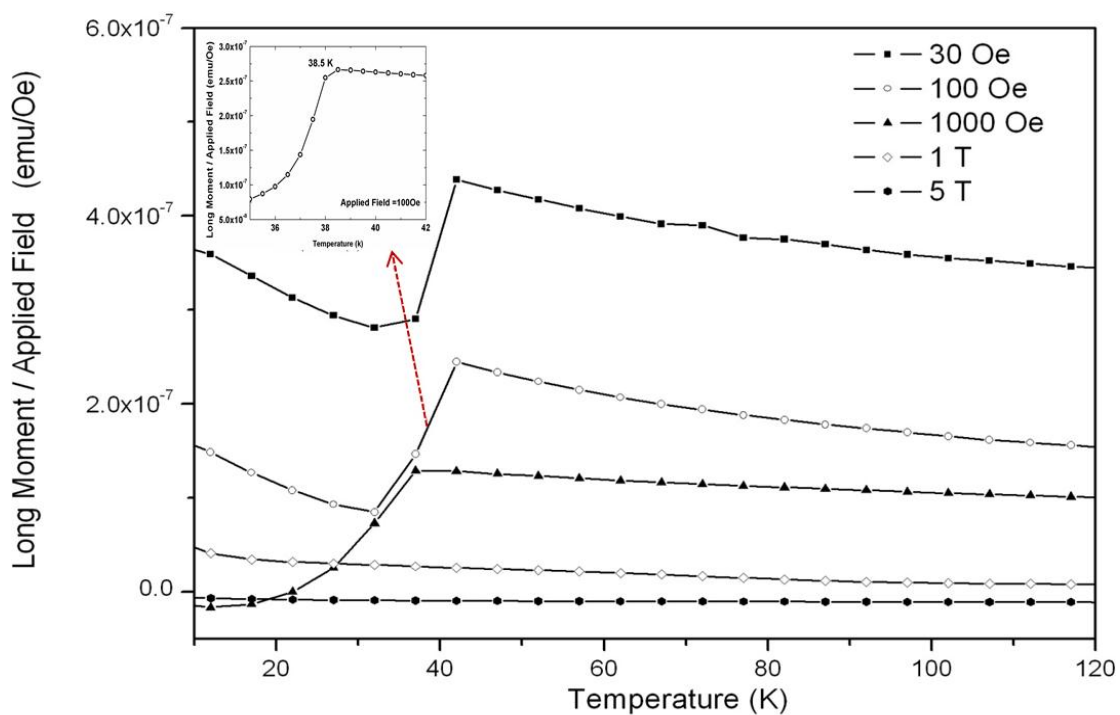


Figure S6: Zero field cooling curves at different applied magnetic fields of 750°C as-synthesized sample.

## Supplementary Material (ESI) for Journal of Materials Chemistry C

This journal is © The Royal Society of Chemistry 2012

### Role of Magnesium in the Fabrication Process.

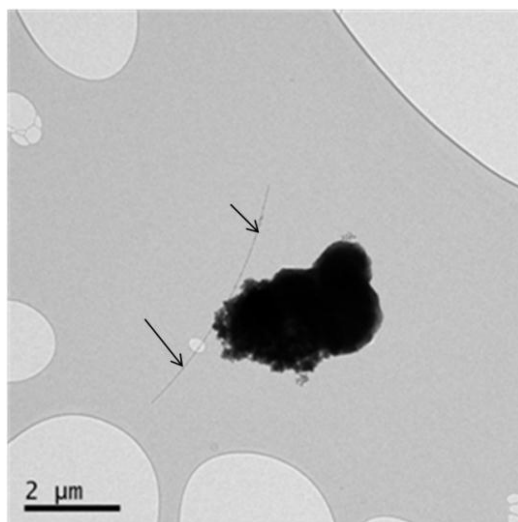


Figure S7: TEM images of nanostructures fabricated from Ni-MCM-41.

## Supplementary Material (ESI) for Journal of Materials Chemistry C

This journal is © The Royal Society of Chemistry 2012

**DC magnetization of the nanostructure fabricated from Ni nanopowder.** The DC magnetization (Figure S8) also indicates the possible existence of superconducting  $\text{MgB}_2$  in the sample synthesized from Ni nanopowder catalyst. The fact that Ni nanopowder generates nanowires with larger diameters compared to the  $\text{MgNi-MCM-41}$  suggests that the existence of the silica template helps to maintain small  $\text{MgNi}$  alloy particles and also likely to physically confine the diameter of nanostructures.

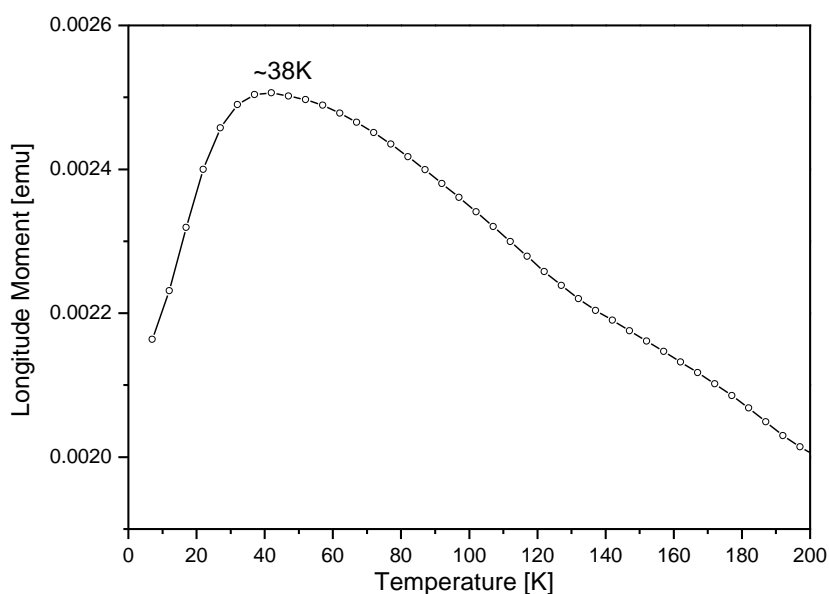


Figure S8: Zero field cooling curve of the nanostructures fabricated from Ni nanopowder.

## Supplementary Material (ESI) for Journal of Materials Chemistry C

This journal is © The Royal Society of Chemistry 2012

### References

1. Y. Yang, S. Lim, C. Wang, D. Harding and G. Haller, *Micropor Mesopor Mat*, 2004, **67**, 245-257.
2. Y. H. Yang, S. Lim, G. A. Du, C. A. Wang, D. Ciuparu, Y. Chen and G. L. Haller, *J. Phys. Chem. B*, 2006, **110**, 5927-5935.
3. H. Scheel, S. Reich, A. C. Ferrari, M. Cantoro, A. Colli and C. Thomsen, *Appl Phys Lett*, 2006, **88**, -.
4. D. R. Tallant, T. L. Aselage, A. N. Campbell and D. Emin, *Phys Rev B*, 1989, **40**, 5649-5656.
5. H. Binnenbruck and H. Werheit, *J Less-Common Met*, 1976, **47**, 91-96.
6. B. M. J.A. Shelnutt, D. Emin, A. Mullendore, G. Slack, and C. Wood, 312.
7. W. Weber and M. F. Thorpe, *J Phys Chem Solids*, 1975, **36**, 967-974.
8. C. L. Beckel, M. Yousaf, M. Z. Fuka, S. Y. Raja and N. Lu, *Phys Rev B*, 1991, **44**, 2535.
9. P. Umari and A. Pasquarello, *Phys Rev Lett*, 2005, **95**.
10. O. Kutsay, C. Yan, Y. M. Chong, Q. Ye, I. Bello, W. J. Zhang, J. A. Zapien, Z. F. Zhou, Y. K. Li, V. Garashchenko, A. G. Gontar, N. V. Novikov and S. T. Lee, *Diam Relat Mater*, 2010, **19**, 968-971.